

SIZE EFFECTS AND LATTICE DISORDER IN GeS₂/CdSe NANOSTRUCTURES

D. Nesheva*, Z. Levi, Z. Aneva

Institute of Solid State Physics, Bulgarian Academy of Sciences, 72 Tzarigradsko Chaussee Blvd., 1784 Sofia, Bulgaria

This article summarizes results on GeS₂/CdSe superlattices (SLs) and composite films (CFs) which are prepared by consecutive thermal evaporation of CdSe and GeS₂ in vacuum. An overall blue shift of the absorption spectra of SLs is observed with decreasing CdSe layer thickness related to a size-induced increase of the optical band gap of CdSe due to one-dimensional carrier confinement in the continuous nanocrystalline CdSe layers. This assumption is proven by the results of photoreflectance measurements. A number of features are observed in the absorption spectra of CFs. They are discussed in terms of three-dimensional carrier confinement and considered as a manifestation of excited electron states in CdSe nanocrystals. Resonant Raman effects are observed in the CFs and related to resonant absorption in the excited electron states. Electronic defects in CdSe nanocrystals of SLs and CFs are investigated by transient and spectral photocurrent investigations. Two wide bands of localized states centred at 0.55 eV and 0.50 eV below the conduction band edge are seen and identified with defects in the nanocrystal bulk and defects at the GeS₂/CdSe interface, respectively. The effect of CdSe nanocrystal incorporation on the level of disorder in the GeS₂ matrix of CFs is also investigated. It is observed that the presence of CdSe nanocrystals with average diameter >2.5 nm in the GeS₂ matrix impedes the photoinduced structural changes in GeS₂.

(Received May 11, 2005; accepted July 21, 2005)

Keywords: CdSe thin films, Photoconductivity, Thermally stimulated currents, Defect states

1. Introduction

Progress in solid state physics was based on the theoretical and experimental studies of single crystals. However, over the past few decades there has been rapidly increasing interest in the preparation of nanometer-sized materials. While non-crystalline solids differ from crystals owing to the lack of long range order (translation symmetry), the main peculiarity of nanomaterials is the presence of a large fraction of atoms located at their surface. The large number of low coordinated atoms at the surfaces of isolated nanocrystals (NCs) or within the grain boundaries of nanosized composite or polycrystalline materials determines many of their physical, chemical and mechanical properties [1]. The quantum confinement results in an increase of the band gap and formation of discrete states at the band edges of semiconductor nanocrystals. The selection rules for optical transitions are relaxed, which leads to increase of transition probabilities for light absorption and emission and makes possible observation of a great number of electron-hole pair transitions. [2,3]. In addition to new physics and chemistry, nanosized materials offer a number of device applications, which can benefit from the size controlled spectral tunability, confinement induced concentration of the oscillator strength (interesting for fabrication of bright light emitting devices with various colors merely by changing NC size) and ultra fast relaxation dynamics (suitable for optical data processing) [4-6].

Bulk composites of Cd chalcogenide (CdSe_xS_{1-x}) semiconductors and silicate glasses (so called semiconductor-doped glasses) have been among the recent focusses of intensive research since they demonstrate a high and fast optical nonlinearity interesting for signal processing or

* Corresponding author: nesheva@issp.bas.bg

designing of optical communication systems. However, because of the broad size distribution, NCs embedded in glass matrices typically do not exhibit sharp absorption features related to size-induced quantization. In contrast, due to the high level of monodispersity, colloidal semiconductor nanoparticles show discrete features [3,7] associated with size quantization and intensive room temperature photoluminescence due to the good passivation of their surface. Together with the quantum confinement effect, the presence of trap levels within the gap and the surface itself strongly affect many properties of semiconductor nanoparticles, particularly II-VI nanocrystals. It has been shown that optical nonlinearity observed in semiconductor doped glasses is connected with carriers trapped in surface defect states which act through the static electric field they create [8]. In addition, the recombination through defect states in the gap of Cd-chalcogenide microcrystals has a strong influence on their photoluminescence [9,10].

In this study we describe the fabrication and characterization of GeS₂/CdSe superlattices (SLs) as well as CdSe nanocrystals embedded in an amorphous GeS₂ thin film matrix (composite films, CFs) prepared using a multilayer deposition technique. Results from transmission, optical absorption (investigated using photocurrent spectroscopy), Raman scattering, d.c. conductivity, photorefectance and transient photoconductivity measurements on these structures are summarized. Size-dependent changes in absorption spectra and resonant Raman scattering results are discussed in terms of one- or three-dimensional carrier confinement and band mixing effects in the valence band of CdSe NCs. The defect state distribution in the gap of CdSe nanocrystalline films is also given. In the end, attention is paid to the effect of CdSe NCs on the photoinduced changes in the GeS₂ thin film matrix.

2. Sample preparation

Multilayer structures were prepared on Corning 7059 glass substrates by consecutive thermal evaporation of CdSe (Merck, Suprapure) and glassy GeS₂ or SiO₂ from two independent tantalum crucibles at a vacuum of $5 \cdot 10^{-4}$ Pa [11]. The nominal film thickness and deposition rate of each material were controlled during deposition by two calibrated quartz monitors. Step-by-step or one-step deposition procedures were applied in fabrication of a given layer in multilayer structures. The former involves rotation of the substrates as they spend only 1/12 part of the cycle over the source. Thus, ten or more 'sublayers', with a nominal thickness of ~0.1-0.25 nm in each step, form the respective layer. In the one-step procedure each film was prepared without interrupting the deposition process. Depending on the thickness of the films and manner of their deposition three kinds of multilayer structures were produced (see Table 1 for details): I) superlattices - step-by-step deposition of both CdSe and GeS₂ films with approximately equal nominal thickness; II) composite films - step-by-step deposition of CdSe and one-step deposition of GeS₂, the nominal thickness of GeS₂ was $d_{GeS_2} = 20 d_{CdSe}$; III) multilayers - one-step deposition of both CdSe and GeS₂ films with equal nominal thickness. High-resolution electron microscopy [11,12] has shown (Fig. 1) that in the second group of samples CdSe layers were not continuous; CdSe nanocrystals with nearly spherical shape were formed whose spatial distribution follows the surface morphology of the underlying GeS₂ film.

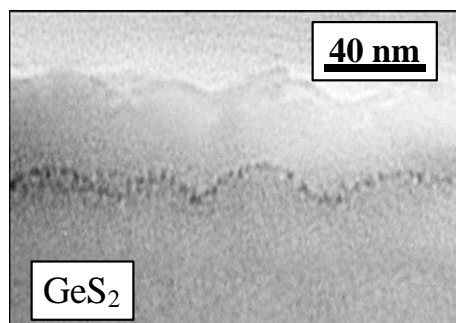


Fig. 1. Electron micrograph of a GeS₂(40 nm)/CdSe(2 nm)/GeS₂(20 nm) three-layer structure.

Table 1. Description of the investigated samples and manner of their preparation. The nominal layer thickness is given in brackets.

Group number	Sample	Manner of layer deposition	
		GeS ₂	CdSe
I. SLs	GeS ₂ (10 nm)/CdSe(10 nm)	step-by-step	step-by-step
	GeS ₂ (6.0 nm)/CdSe(5.0 nm)	step-by-step	step-by-step
	GeS ₂ (4.0 nm)/CdSe(4.0 nm)	step-by-step	step-by-step
	GeS ₂ (3.5 nm)/CdSe(3.5 nm)	step-by-step	step-by-step
	GeS ₂ (2.5 nm)/CdSe(2.5 nm)	step-by-step	step-by-step
II. CFs	GeS ₂ (100 nm)/CdSe(5.0 nm)	one step	step-by-step
	GeS ₂ (60 nm)/CdSe(3.0 nm)	one step	step-by-step
	GeS ₂ (40 nm)/CdSe(2.0 nm)	one step	step-by-step
	GeS ₂ (20 nm)/CdSe(1.0 nm)	one step	step-by-step
III.	GeS ₂ (5.0 nm)/CdSe(5.0 nm)	one step	one step
	GeS ₂ (2.5 nm)/CdSe(2.5 nm)	one step	one step

3. Size-dependent optical band gap

3.1 Superlattices

Fig. 2 [13] shows absorption spectra obtained using standard spectral photocurrent measurements of GeS₂/CdSe SLs having four different layer thicknesses. No appreciable difference in the shape of the different spectra is observed up to 2.6 eV at which the contribution of GeS₂ in the SL absorption becomes significant and causes a slight change in the curves' slope. The absorption spectra are featureless but they are blue-shifted with decreasing layer thickness. The results are similar to those obtained in SiO_x/CdSe and ZnSe/CdSe SLs [14,15] and have been attributed [13] to one-dimensional carrier confinement in continuous nanocrystalline CdSe layers (along the SL axis) rather than three-dimensional confinement in each separate nanocrystal.

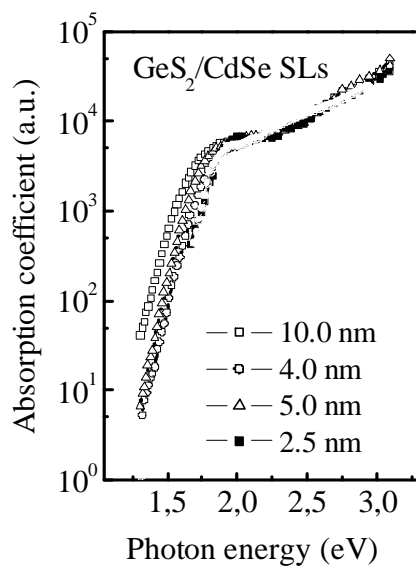


Fig. 2. Optical absorption spectra of GeS₂/CdSe SLs having four different layer thicknesses.

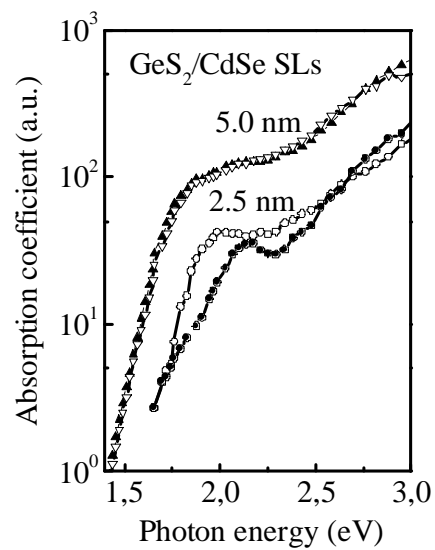


Fig. 3. Optical absorption spectra of '2.5 nm' and '5.0 nm' SLs and multilayer structures with the same layer thickness deposited in step-by-step (open symbols) or one step (solid symbols) manner.

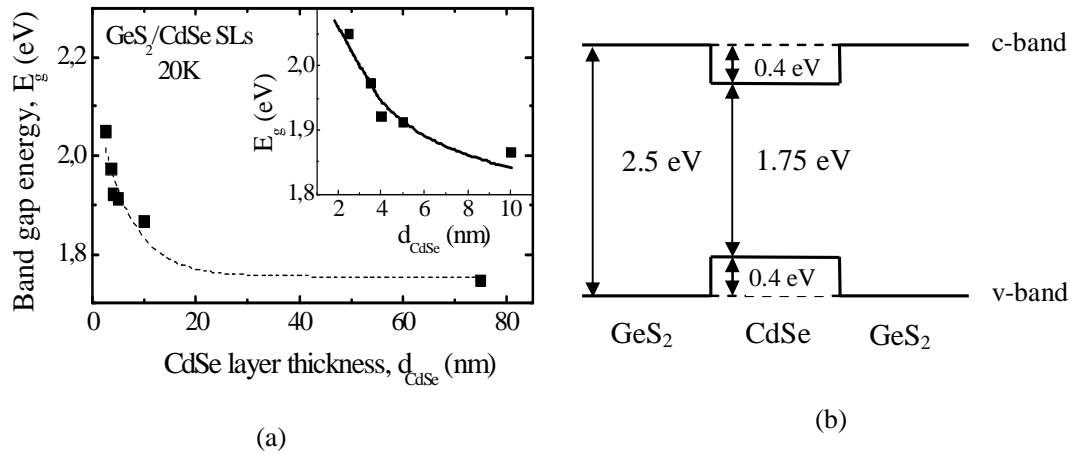


Fig. 4. (a) Band gap energies of CdSe/GeS₂ superlattices in dependence of the CdSe sublayer thickness d_{CdSe} at 20 K. Inset: the E_g data (symbols) are compared with the calculated widening of the optical band gap of CdSe sublayers in these SLs; (b) schematic band diagram of GeS₂/CdSe superlattices.

Absorption spectra of ‘2.5 nm’ and ‘5.0 nm’ SLs are shown in Fig. 3 [12] together with spectra of multilayer structures with the same layer thickness but deposited in the one step manner (Table 1, third group of samples). No difference is seen in the spectra of both ‘5 nm’ samples which indicates that, though the interface roughness in ‘5 nm’ samples from the third group should be higher than in the first group ones, most likely their CdSe layers are still continuous. However, the spectrum of third group ‘2.5 nm’ sample is quite different; a maximum at ~2.1 eV is seen, which is characteristic for CFs (see Fig. 6 below) rather than for SLs. The observation has been explained assuming that when very thin CdSe layers are deposited on an insufficiently smooth GeS₂ surface (due to the applied one-step deposition approach) they are not continuous but island type with approximate island radius of ~2.2 nm (corresponding to an optical gap of 2.1 eV, determined from Fig. 9 in Ref. 3). Should this be the case, the lack of distinct features in absorption spectra of these samples implies a wide size distribution of CdSe islands. The appearance of such features in CF spectra (see Fig. 6 and the related discussion) implies that the increase of the surface roughness results in narrowing of the NC size distribution. It seems that at room substrate temperature and thickness ratio of $d_{GeS_2}/d_{CdSe} = 20$ the surface roughness of the ‘matrix’ layers is great enough to ensure formation of nearly monodisperse CdSe nanocrystals.

Low temperature photoreflectance measurements at 20 K have been performed [16] on GeS₂/CdSe SLs, with layer thickness varying from 2.5 to 10 nm. In Fig. 4a, the energy dependence of the optical band gap of the SLs measured at 20 K is presented. It is seen that the band gap of SLs increases up to a maximum of 175 meV with reducing the layer thickness down to 2.5 nm. This dependence is a direct experimental evidence of the assumed low dimensionality of these structures. Calculations were performed by considering one dimensional rectangular potential wells for both, electrons and holes, in the CdSe layers and using effective masses of $m_e^* = 0.12 m_e$, for the electrons, and $m_{hh}^* = 0.9 m_e$, for the heavy holes (m_e is the free electron mass) [17]. The potential well depth for both kinds of charge carriers was varied between 0.2 and 0.6 eV. The best agreement between the experimental data and the calculated size dependence of the energy gap has been achieved for equal depths of 0.4 eV of both wells and it is shown in the inset of Fig. 4a. Based on these results, a schematic band diagram of the GeS₂/CdSe SLs has been suggested which is presented in Fig. 4b.

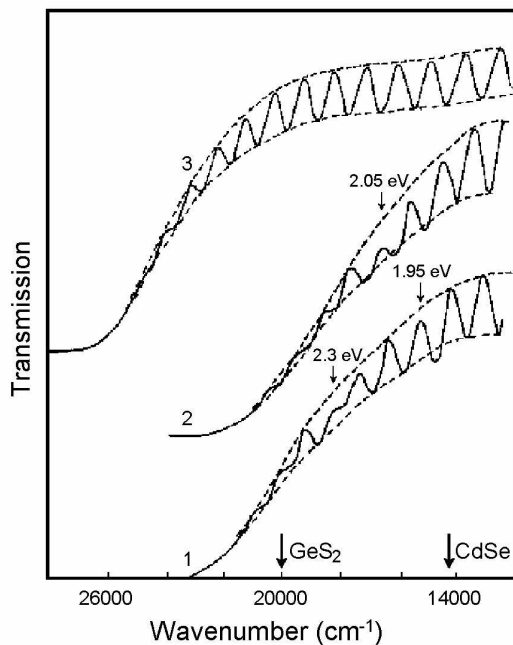


Fig. 5. Optical transmission spectra of two GeS₂/CdSe composite films having CdSe nominal thickness of 5 and 3 nm (curves 1 and 2, respectively) and a single GeS₂ thin film (curve 3). The arrows denote bulk optical band gaps of CdSe ($E_g=1.75$ eV) and GeS₂ ($E_g=2.5$ eV). Regular interference is observed in GeS₂ spectrum while some features are seen in the spectra of composite films.

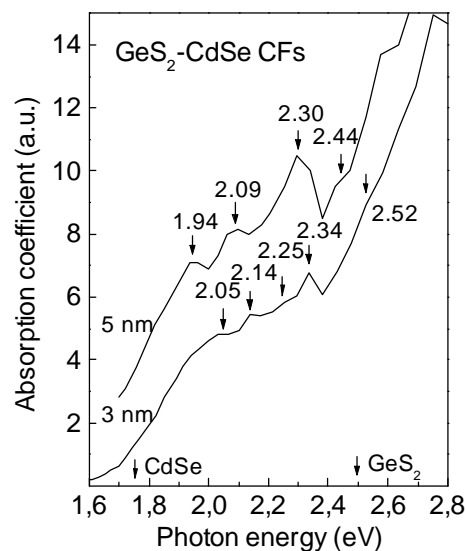


Fig. 6. Optical absorption spectra of two composite films with nominal CdSe thickness of 3 and 5 nm. The arrows and numbers identify the bulk optical band gaps of CdSe and GeS₂ as well as energy positions of all features observed.

3.2 Composite films

Optical transmission spectra of a single GeS₂ thin film and two GeS₂/CdSe composite films having CdSe nominal thickness of 3 and 5 nm are shown in Fig. 5 [13]. The arrows depict bulk optical band gaps of CdSe ($E_g=1.75$ eV) and GeS₂ ($E_g=2.5$ eV) single layers produced at same deposition conditions as the respective layer in the CFs. Regular interference fringes in the spectra were typical for GeS₂ single layers as well as for GeS₂/CdSe SLs (not shown here). Since in the CFs the total thickness of GeS₂ is 20 times the thickness of CdSe, GeS₂ dominates transmission of these films. However, some features are seen in their transmission spectra, which appear at energies lower than E_g of GeS₂ but higher than the optical band gap of bulk CdSe. Since there are no peculiarities in the GeS₂ spectrum, it is anticipated that these are due to light absorption in CdSe nanoparticles and imply that, as expected, the energy gap of CdSe nanocrystals is higher than that of bulk CdSe. A second feature at ~ 2.3 eV is also seen in the transmission spectrum of the '5 nm' composite film. Although these features can be seen in the transmission spectrum they are obscured to some extent by the thin-film optical interference.

In order to measure absorption with greater accuracy, photocurrent measurements have been carried out on GeS₂/CdSe CFs, as well [13]. Carrier transport studies have confirmed [11] that in composite films charge transport, in the layer plane, involves networks of contacting CdSe nanocrystals, which made possible to study absorption of the quasi-isolated CdSe NCs by means of spectral photocurrent measurements. The measurements of photoconductivity of separately prepared CdSe and GeS₂ films have shown that photoconductivity of GeS₂ is more than 100 times smaller than that of CdSe. Also it can be seen from the transmission spectrum of the GeS₂ film shown in Fig.5 that absorption of GeS₂ becomes appreciable only at energies above 2.5 eV. Therefore, at lower energies the CF (and SL) spectra have been related only to absorption in CdSe.

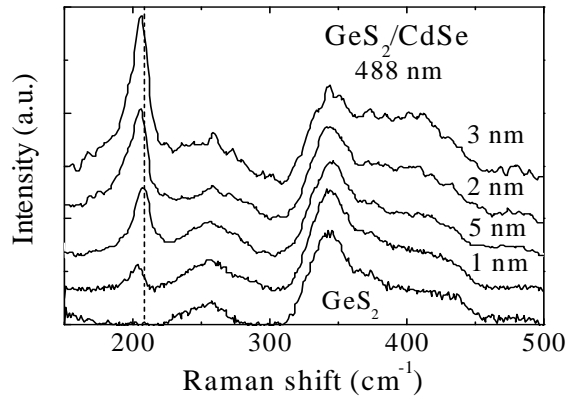


Fig. 7. Room temperature Raman scattering spectra of GeS_2/CdSe CFs for four values of nominal thickness d_{CdSe} of the CdSe layers and of an a- GeS_2 single layer, excited by the 488 nm Ar^+ laser line. The vertical dotted line has been inserted to show the shift towards the lower frequencies of the CdSe 1LO phonon band with decreasing d_{CdSe} . All spectra correspond to the same intensity scale, but they are vertically displaced for clarity.

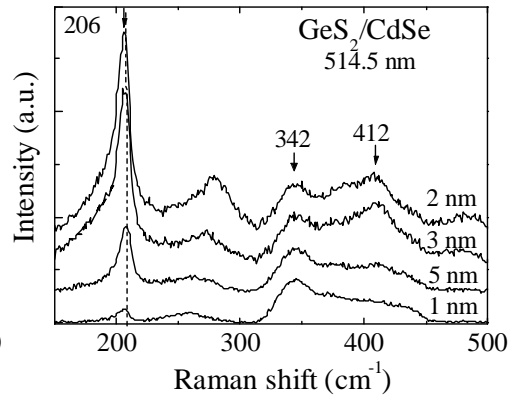


Fig. 8. Room temperature Raman scattering spectra of a- GeS_2 - c-CdSe composite films for four values of nominal thickness d_{CdSe} of the CdSe layers, excited by the 514.5 nm Ar^+ laser line. All spectra correspond to the same intensity scale, but they are vertically displaced for clarity.

Fig. 6 shows absorption spectra of two composite films with nominal CdSe thickness of 3 and 5 nm obtained by spectral photocurrent measurements, which exhibit some features at high energies. We have made [13] a careful comparison of the transmission fringe minima (Fig.5) with the positions of the features in Fig. 6, which we ascribe to optical transitions. While there are some correlations, many of the features have no analogue in the optical absorption spectrum and vice versa, and thus the following assignments have been made. The maximum at the lowest energy in the absorption spectrum defines the NC energy gap and corresponds to the $1S_{3/2}-1S_e$ electron transition in CdSe quantum dots [3]. Using the NC energy gap *vs.* size dependence [Fig. 9 in Ref.3], values of ~ 2.5 nm and ~ 3.3 nm have been obtained for the average radius of CdSe nanocrystals in the nominally '3 nm' and '5 nm' samples, respectively. Since the NC radii determined are smaller than the exciton Bohr radius in CdSe (5.6 nm [2]), a strong confinement situation can be expected, in which both carriers are independently confined.

It is known [2,3] that due to the valence band degeneracy in CdSe mixing between the bulk light hole, heavy hole and spin-orbit split-off valence subbands occurs which is weak in bulk excitons but significant in quantum dots. As result, discrete features should appear in absorption of monodispersive CdSe NCs related to excitons. Well expressed features have been observed in absorption of colloidal CdSe NCs but not in NCs embedded in glass matrices. The discrete features we observed in the '5 nm' and '3 nm' GeS_2/CdSe CF absorption have been associated with size quantization and considered as an indication of a high level of sample monodispersity. In a detailed study of excitons in colloidal CdSe quantum dots the intensity calculations and experimental results have shown [7] that $n_h S_{3/2}-1S_e$, $n_h S_{1/2}-1S_e$ and $1P_{3/2}-1P_e$ transitions account for most of the observed features in the spectra. In Ref.13 the positions of the features seen in the 'photocurrent' absorption spectra of '3 nm' and '5 nm' GeS_2/CdSe CFs have been compared with the energy of some excitons observed in colloidal CdSe quantum dots [7]. An excellent agreement has been between the measured and expected energy of all transitions. These results show that: first, CdSe NCs in a- GeS_2 matrix produced by the applied multilayer approach have a narrow size distribution and, second, easy and successful investigation of excitons in photoconductive semiconductor quantum dots can be performed by means of spectral photocurrent measurements.

Raman scattering spectra of these films have been measured in the temperature range 20 K to 293 K using three Ar⁺ laser lines for the excitation and studied with emphasis to the position and intensity of the longitudinal optical phonons of CdSe [18]. A shift to lower frequencies has been observed in these phonons (see Fig. 7), which increases with decreasing CdSe layer thickness. The result is expected and indicates three-dimensional localization of longitudinal optical (LO) phonons in CdSe nanocrystals. On the other hand, resonant Raman effects have been observed as the phonon intensity depends strongly on the nominal CdSe layer thickness, excitation light (see Fig. 8) and temperature. These results confirm the above made conclusion about formation of high quality CdSe nanocrystals in the amorphous GeS₂ thin film matrix and have been interpreted [18] in terms of resonant absorption in exciton electronic states of CdSe nanocrystals. Such an exciton related resonance has been observed for the first time in II-VI semiconductor nanocrystals.

4. Defect states in CdSe nanocrystals

Electronic defects in CdSe nanocrystals of GeS₂/CdSe superlattices and composite films have been investigated by transient photocurrent (TPC) spectroscopy [19]. A wide band of localized states centred at ~0.55 eV below the conduction band edge is seen in Fig. 9 in both groups of samples. It has been identified with defects in the nanocrystal bulk. A band at ~0.7 eV below the conduction band has been well resolved in SiO_x/CdSe samples [20] but not seen in GeS₂/CdSe films. As this feature has been ascribed [20] to defects at the CdSe-CdSe interface, a lower density of such defects is assumed in the latter case. In GeS₂/CdSe samples a new band located at 0.50 eV below the conduction band has appeared. It has been attributed to defects at the GeS₂-CdSe interface. Optical absorption measurements reveal an exponential absorption tail related to electronic transitions from defect states in the valence band tail to the lowest extended states in the conduction band. It has been obtained [19] that defect concentration above the valence band of CdSe nanocrystals in GeS₂/CdSe samples is lower than in SiO_x/CdSe ones. Steady-state photoconductivity of GeS₂/CdSe samples has shown that at low temperatures the mobility-lifetime product in CdSe nanocrystals decreases with decreasing nanocrystal size. This observation is related to deep defects at the interface of CdSe nanocrystals and reflects the increasing surface to volume ratio.

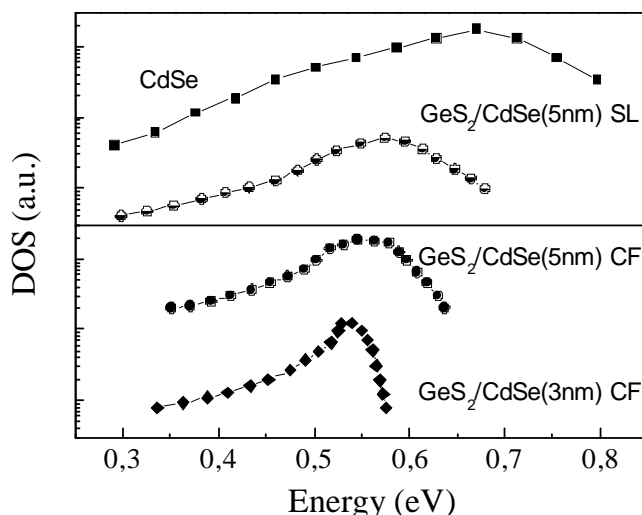


Fig. 9. Density of defect states distribution (DOS) from top down: a CdSe single layer, a '5 nm' GeS₂/CdSe superlattice, '5 nm' and '3 nm' GeS₂/CdSe composite films. The energy is given with respect to the conduction band edge. All spectra correspond to the same scale. Although the plots shown are only a relative measure of the DOS, they may be used to compare the magnitudes and energy positions of defects.

5. Photobleaching in composite films

Photobleaching has been studied in GeS_2/CdSe composite films in order to explore the influence of CdSe nanocrystals on the reversible photoinduced structural changes in the GeS_2 thin film matrix [21]. Optical transmission spectra of GeS_2/CdSe CFs and a GeS_2 single layer, measured in the region 300-700 nm before and after light illumination, are shown in Fig.9 and 10, respectively. The peculiarities in the optical transmission spectra of GeS_2/CdSe CFs discussed above are well seen at energies lower than the optical band gap of GeS_2 but higher than the optical band gap of bulk CdSe; no such peculiarities are observed in the spectrum of GeS_2 single layer. The energy positions of the features coincide with the expected optical band gap of CdSe nanocrystals for the corresponding nominal thickness of CdSe layers. The observation proves the existence of nanocrystals of various sizes in this particular series of samples. The comparison of the spectra shown in Figs. 9 and 10 indicates that the observed photoinduced blue shift of the absorption edge in CFs with nominal layer thickness of 2 nm and 5 nm is smaller than that in the GeS_2 single layer and decreases with decreasing CdSe nanocrystal size. In the films with nominal layer thickness of 1 nm, the photobleaching effect does not differ appreciably from the effect observed in the GeS_2 single layer.

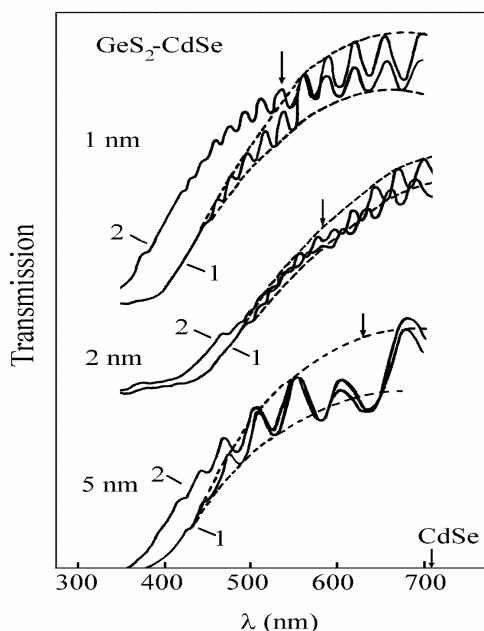


Fig. 10. Optical transmission spectra of GeS_2/CdSe composite films before (1) and after (2) illumination with a high pressure Hg lamp for 45 min. Peculiarities are seen, denoted by arrows, at energies higher than the optical bandgap, of bulk CdSe.

Cross-sectional electron micrographs of SiO_x/CdSe CFs have revealed [22] that at CdSe nominal thickness ≥ 2 nm nanoparticles have a crystalline structure. It is known that in amorphous materials, in particular in a- GeS_2 , the network is more flexible than that of crystalline materials. Therefore, it has been assumed that in the interface region the GeS_2 network is properly arranged to minimize the internal strains in the system and this arrangement differs from that of a single GeS_2 layer. Thus, the observed decrease of photobleaching has been related to the influence of the interfaces on the ordering of the amorphous matrix. In the '5 nm' layers the surface-to-volume ratio is relatively low and the effect of nanocrystals is relatively weak. In the '2 nm' GeS_2/CdSe composite films this ratio is significantly higher, which is most probably the reason for the smallest blue shift observed in these composite films. Having in mind the great number of nanoparticles that form a CdSe sublayer, one could expect a very small blue shift in the '1 nm' CFs. However, the observed photobleaching in the '1 nm' GeS_2/CdSe composite films is as great as in the GeS_2 film. In

order to understand this result, one should take into account that 1 nm CdSe nanoparticles are amorphous rather than crystalline [22] and their size is very small (in the scale of the medium range order in GeS₂). Most likely, the flexible structure of these quite tiny CdSe nanoparticles does not appreciably affect the light induced bond reconstruction. The size of 2.5 nm must be compared with the size of CdSe nano-crystals reported in [23, 24], 65-89 nm, which represents in fact a mixture of h.c.p. and f.c.c. phases.

6. Conclusions

Continuous and 'island' type CdSe nanocrystalline layers sandwiched between GeS₂ amorphous thin and ultra thin films have been produced using a multilayer approach, in which surface roughness of GeS₂ films played an important role in CdSe nanoparticle formation. Both the transmission and spectral photocurrent measurements applied to study optical absorption of all samples have shown a small overall blue shifts with decreasing CdSe layer thickness of superlattices, which has been related to a size-induced increase of the optical band gap in continuous nanocrystalline CdSe layers. This suggestion has been confirmed by the results from the photoreflectance measurements. The features observed in the absorption spectra of composite films containing CdSe nanocrystals with average radius of ~2.5 nm and ~3.3 nm have been related to three-dimensional carrier confinement in each separate CdSe nanocrystal of 'island' type films. The observation of such features has indicated that at a thickness ratio of $d_{GeS_2}/d_{CdSe} = 20$ and one step deposition of GeS₂, the surface roughness of GeS₂ 'matrix' layers is great enough to ensure formation of nearly monodisperse CdSe nanocrystals.

The TPC results support the view that transport in CdSe nanocrystalline films is strongly influenced by the presence of lattice disorder and by other localised states associated with defects, such as surface states at the nanocrystal boundaries.

The investigation of the photobleaching in GeS₂/CdSe composite films has indicated that the presence of CdSe nanocrystals with average diameter >2.5 nm leads to an appreciable change of the lattice disorder in the GeS₂ matrix and, thus, impedes photoinduced structural changes in GeS₂, while nanocrystals having smaller sizes do not significantly affect the photoinduced changes in the local order of the matrix material.

Acknowledgements

This work has been supported by the Bulgarian Ministry of Education and Science under Grant F 1306. The authors are very grateful to Dr. C. Raptis, Dr. S. Reynolds, Dr. C. Main, Dr. D. Papadimitriou for the fruitful cooperative investigations on GeS₂/CdSe SLs and CFs.

References

- [1] S. Veprek, *Thin Solid Films* **297**, 145 (1997).
- [2] A. I. Ekimov, F. Hache, M. C. Schanne-Klein, D. Ricard, C. Flytzanis, I. A. Kudryavtsev, T. V. Yazeva, A. V. Rodina, Al. L. Efros, *J. Opt. Soc. Am. B*, **10**, 100 (1993).
- [3] V. I. Klimov, in *Handbook of Nanostructured Materials and Nanotechnology*, ed. H. S. Nalwa, Academic Press, San Diego (2000), Vol. **4**, p.451.
- [4] A. P. Alivisatos, *MRS Bulletin* **23**, 18 (1998).
- [5] M. Grätzel, in *Handbook of Nanostructured Materials and Nanotechnology*, ed. H. S. Nalwa, Academic Press, San Diego (2000), Vol. **3**, p.527.
- [6] A. Sombra, *Solid State Commun.* **88**, 305 (1993).
- [7] D. Norris, M. Bawendi, *Phys. Rev. B*, **53**, 16338 (1996).
- [8] C. Flytzanis, D. Ricard, M. C. Schanne-Klein, *J. Luminescence* **70**, 212 (1996).
- [9] D. Nesheva, C. Raptis, Z. Levi, Z. Popovic, I. Hinic, *J. Luminescence* **82**, 233 (1999) and reference therein.
- [10] P. Nemeč, P. Maly, *J. Appl. Phys.* **87**, 3342 (2000).

- [11] D. Nesheva, in Handbook of Surfaces and Interfaces of materials, ed. H.S. Nalwa, Academic Press, San Diego (2001), Vol. **3**, p.239.
- [12] D. Nesheva, H. Hofmeister, Z. Levi, Z. Aneva, Vacuum **65**, 109 (2002).
- [13] D. Nesheva, Z. Levi, Z. Aneva, I. Zrinscak, C. Main, S. Reynolds, J. Nanoscience & Nanotechnology **3**, 645 (2002).
- [14] D. Nesheva, Z. Levi, Z. Aneva, V. Nikolova, H. Hofmeister, J. Phys.: Condens. Matter. **12**, 751 (2000).
- [15] D. Nesheva, H. Hofmeister, Z. Levi, I. Bineva, in Nanostructured Materials: Selected synthesis methods and application, eds. P. Knauth and J. Schoonmann, Kluwer Academic Publishers, Boston, USA, (2002), p.115.
- [16] G. Manolis, D. Papadimitriou, D. Nesheva, to be published in Proc. E-MRS Symposium, 2005.
- [17] Landolt-Börnstein, Numerical Data and Functional Relationships in Science and Technology, ed. O. Madelung, Springer Verlag, Berlin-Heidelberg-New York 1982, group III, vol. 17B, p.202.
- [18] C. Raptis, D. Nesheva, Y. C. Boulmetis, Z. Levi, Z. Aneva, J. Phys.: Condens. Matter. **16**, 8221 (2004).
- [19] Z. Aneva, D. Nesheva, C. Main, S. Reynolds, J. Optoelectron. Adv. Mater. 2005, in press.
- [20] D. Nesheva, S. Reynolds, C. Main, Z. Aneva, Z. Levi, phys. stat. sol. (a) **202**, 1081 (2005).
- [21] Z. Levi, in Proc. 5th Workshop on Nanosci. and Nanotechnol., Sofia, November 2003, Eds. E. Balabanova and I. Dragieva, Heron press, Nanoscience and Nanotechnology **4**, 69 (2004).
- [22] D. Nesheva, J. Optoelectron. Adv. Mater. **3**, 885 (2001).
- [23] S. Antohe, L. Ion, V. A. Antohe, J. Optoelectron. Adv. Mater. **5**(4), 801 (2003).
- [24] L. Ion, V. A. Antohe, S. Antohe, J. Optoelectron. Adv. Mater. **7**(4), 1847 (2005).